

## A single-cell drug efflux assay in bacteria by using a directly accessible femtoliter droplet array<sup>†</sup>

Ryota Iino,<sup>\*ab</sup> Kohei Hayama,<sup>c</sup> Hiromi Amezawa,<sup>a</sup> Shouichi Sakakihara,<sup>c</sup> Soo Hyeon Kim,<sup>ab</sup> Yoshimi Matsumono,<sup>c</sup> Kunihiro Nishino,<sup>c</sup> Akihito Yamaguchi<sup>c</sup> and Hiroyuki Noji<sup>ab</sup>

Received 23rd April 2012, Accepted 7th June 2012

DOI: 10.1039/c2lc40394c

Active efflux of drugs, such as antibiotics, from a cell is one of the major mechanisms that cause multi-drug resistance in bacteria. Here we report a method to assess drug efflux activity in individual *Escherichia coli* cells enclosed and isolated in a directly accessible femtoliter droplet array with a fluorogenic compound. The inhibitory effect of a chemical compound on an exogenously expressed efflux pump system from pathogenic bacteria was easily detected at the single-cell level. We also present a proof-of-principle experiment to screen for the gene encoding a drug efflux pump by collecting individual droplets containing single cells in which the drug efflux activity was restored after introduction of the exogenous gene from pathogenic bacteria. Our approach will be a useful tool to screen novel pump inhibitors and efflux pump genes, and to overcome infectious diseases caused by multi-drug-resistant bacteria.

### Introduction

The recent increase in multi-drug resistance in clinically isolated bacteria is a major problem in infection control.<sup>1</sup> The major causes of bacterial drug resistance can be divided into 4 categories: suppression of drug influx into the cell by decreased expression of membrane channel proteins, inactivation of drugs by enzymes inside the cell, mutations in the target proteins of drugs, and active efflux of drugs from the cell by increased expression of efflux pump systems. The AcrAB-TolC system is a multicomponent pump complex that is responsible for both the intrinsic and acquired drug tolerance of Gram-negative bacteria such as *Escherichia coli* (*E. coli*) and *Salmonella enterica* (*S. enterica*).<sup>2,3</sup> The AcrAB-TolC system recognises a wide variety of compounds as substrates and pumps out antibiotics, dyes, and detergents, driven by the proton-motive force across the inner membrane. AcrA is a membrane fusion protein,<sup>4</sup> AcrB an inner membrane protein,<sup>5</sup> and TolC an outer membrane protein.<sup>6</sup> A homolog of the AcrAB-TolC, MexAB-OprM and MexXY-OprM systems elicits multi-drug resistance in clinically isolated *Pseudomonas aeruginosa* (*P. aeruginosa*).<sup>7–11</sup>

Drug resistance caused by active efflux is conventionally assessed by measuring the minimal inhibitory concentration

(MIC) of the drug against bacterial growth. This is an indirect method, and in principle, cells can grow by mechanisms other than active efflux. Direct evaluation of the efflux activity of bacteria is awaited. To achieve this, we have recently developed an optical imaging-based efflux assay by combining a microfluidic device with a fluorogenic compound, fluorescein-di- $\beta$ -D-galactopyranoside (FDG).<sup>12,13</sup> Due to the broad substrate specificity of multi-drug efflux pump systems,<sup>14</sup> FDG and fluorescein, the hydrolysed fluorescent product of FDG by  $\beta$ -galactosidase in the cytoplasm of *E. coli*, can act as substrates for AcrAB-TolC and its homologs, and enable the detection of efflux activity with fluorescence measurement in the microfluidic channel. This microchannel-based efflux assay is simple and efflux activity can be rapidly evaluated. However, owing to the relatively large volume of the microfluidic channel, an ensemble of cells is required to obtain results, and the assay at the single-cell level is difficult. Furthermore, once introduced into the channel, the cells cannot be collected and used for subsequent analysis.

Single-cell assays and analyses are powerful approaches to capture the variations detected in individual cells, such as the expression levels of proteins and copy number of genes.<sup>15</sup> The results from these approaches will not suffer from the limitations associated with ensemble-averaged data from many cells. Microfabricated devices have extensively contributed to the development of high-throughput single-cell analysis. Most target cells are eukaryotic cells, such as mammalian cells and yeasts,<sup>16–18</sup> because their relatively large size (several to several tens of micrometers) makes their handling easier than that of smaller ones, namely, bacteria. A limited number of studies have used microdevices for single-cell analysis of bacteria.<sup>19–23</sup> Furthermore, in many single-cell assays based on microfluidic channels and

<sup>a</sup>Department of Applied Chemistry, University of Tokyo, 7-3-1 Hongo, Bunkyo-ku, Tokyo 113-8656, Japan. E-mail: iino@appchem.t.u-tokyo.ac.jp; Fax: +81-3-5841-1872; Tel: +81-3-5841-7241

<sup>b</sup>CREST, Japan Science and Technology Agency, Sanbancho 5, Chiyoda-ku, Tokyo 102-0075, Japan

<sup>c</sup>Institute of Scientific and Industrial Research, Osaka University, 8-1 Mihogaoka, Ibaraki, Osaka 567-0047, Japan

† Published as part of a themed issue dedicated to Emerging Investigators.

valves or microdroplets generated in a microchannel, the closed nature of the systems makes the collection of the cells from the device and their subsequent use difficult.

We have previously developed a water-in-oil, directly accessible femtoliter microdroplet array, formed on a hydrophilic-in-hydrophobic micropatterned surface and shown its application in single-molecule enzyme assays.<sup>24</sup> In contrast to microdroplet generation with constant flow in microchannels, droplet array formed and fixed on the surface makes it easy to monitor the same droplets for a long time. Furthermore, no equipment for flow control, such as pumps and valves, is required. In the present study, we applied this droplet array to a single-cell assay to assess the drug efflux activity of bacteria. By enclosing and isolating individual bacteria in a femtoliter droplet, we can easily detect the efflux activity of individual cells. The effect of an efflux pump inhibitor could be easily assessed with this assay. We found that the efflux-active phenotype appeared within a few hours after introduction of the exogenous gene encoding an efflux pump system into the efflux-deficient strain. Moreover, with the advantage of accessibility to individual droplets, an efflux-active single cell in a droplet can be easily collected under an optical microscope, and can be used for subsequent culture and gene analysis. Multi-drug resistant bacteria may harbour many putative genes responsible for active drug efflux. Our phenotype-based approach will be a potent tool to screen for novel pump inhibitors and pump genes and to overcome infectious diseases caused by multi-drug resistant bacteria.

## Experimental

### Bacterial strains, plasmids, and chemicals

*E. coli* MG1655 wild-type strain, and its efflux-pump-gene deletion mutants,  $\Delta acrB$  ( $\Delta B$ ),  $\Delta tolC$  ( $\Delta C$ ), and  $\Delta acrB\Delta tolC$  ( $\Delta B\Delta C$ ), were used.<sup>25</sup> Strains harbouring the vector plasmid pMMB67HE or pTH18kr were grown in medium containing 100  $\mu$ g mL<sup>-1</sup> ampicillin or 50  $\mu$ g mL<sup>-1</sup> kanamycin (Sigma-Aldrich, USA), respectively, to ensure plasmid retention. Isopropyl- $\beta$ -D-galactopyranoside (IPTG; Sigma-Aldrich, USA) was added to the medium for  $\beta$ -galactosidase and plasmid-mediated pump induction. Fluorescein-di- $\beta$ -D-galactopyranoside (FDG; Marker Gene Technologies, USA) was used as a substrate for the efflux pump. D13-9001 (Daiichi Sankyo, Japan) was used as an efflux pump inhibitor.<sup>26</sup>

### Preparation of the hydrophilic-in-hydrophobic micropatterned surface

A hydrophobic polymer of carbon-fluorine (CYTOP; Asahi-Glass, Japan) was spin-coated on a cleaned coverglass (30 mm in diameter; Matsunami, Japan) at 2000 rpm for 30 s and then baked for 1 h at 180 °C. Photolithography was performed with a high-viscosity photoresist (AZP4903; AZ Electronic Materials, Japan) because the CYTOP-coated surface had very low friction and could not be completely covered with a low-viscosity photoresist. The resist-patterned substrate surface was dry-etched with O<sub>2</sub> plasma using a reactive ion-etching system (RIE-10NR; Samco, Japan) to expose the hydrophilic SiO<sub>2</sub> glass surface. The diameter of the SiO<sub>2</sub> surfaces was 10  $\mu$ m, and the center-to-center distance was 15  $\mu$ m or 20  $\mu$ m. The thickness of

the CYTOP layer was 1  $\mu$ m as measured by a laser microscope (VF-7500; KEYENCE, Japan).

### Microdroplet array formation and bacterial enclosure

The hydrophilic-in-hydrophobic micropatterned coverglass was attached to the bottom of a perforated petri dish (35 mm in diameter) (Fig. 1A) and covered with medium containing bacteria (Fig. 1B). A fluorinated oil (Fluorinert FC40; Sigma-Aldrich, USA), which has a higher density than water, was then flowed into the medium near the substrate surface. The hydrophilic SiO<sub>2</sub> glass surface retained the medium and bacteria, while the hydrophobic surface was covered with oil. As a result, many microdroplets containing single or multiple bacteria were simultaneously formed.

### General method of single-cell efflux assay

Overnight cultures of strains in Luria-Bertani (LB; Becton Dickinson and Company, USA) medium at 37 °C were inoculated in 2 mL of fresh medium and incubated at 37 °C on a shaker until the culture reached a turbidity at 600 nm of 0.6. IPTG (1 mM) was added to induce  $\beta$ -galactosidase.

The bacterial cultures (450  $\mu$ L) were mixed with 50  $\mu$ L of FDG solution (1 mg mL<sup>-1</sup>) and used for droplet array formation. After incubation for 15 min at room temperature, the droplet

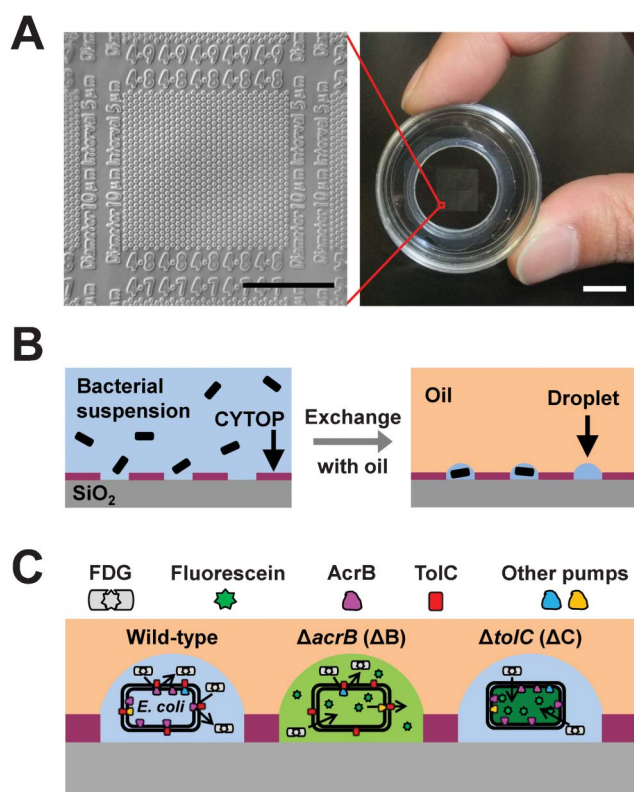


**Fig. 1** Image of the device and principle of the single-cell drug efflux assay. (A) Image of the device for single-cell drug efflux assay (right). Scale bar, 10 mm. Microscopic image of the hydrophilic-in-hydrophobic micropatterned surface (left). Scale bar, 200  $\mu$ m. (B) Procedure for bacterial enclosure into a femtoliter droplet array. (C) Schematic drawing of the principle of assay.

array was observed under an optical microscope (BZ-8000; KEYENCE, Japan) equipped with an objective lens (CFI Plan Apo 20  $\times$ , NA0.75; Nikon). Eight-bit grayscale *epi*-fluorescence (excitation: 450–490 nm; emission: 510–560 nm) and phase contrast images were sequentially obtained with a cooled CCD camera. Individual cells were visually identified and their position in the fluorescence image was manually determined using the phase contrast image. Fluorescence intensity of individual cells and droplets were measured using ImageJ software. The assays were performed at least 2 times for individual experimental conditions, and more than 100 cells were analysed for each experimental condition in a single assay.

### Effect of an efflux pump inhibitor, D13-9001

The vector plasmid pMMB67HE was recombined with the efflux pump genes *mexAB-oprM* from *P. aeruginosa* (pMMB67HE::*mexAB-oprM*)<sup>27</sup> and introduced into a  $\Delta$ BAC double-knockout strain to generate  $\Delta$ BAC/pMMB67HE::*mexAB-oprM*. Ampicillin (100  $\mu$ g mL<sup>-1</sup>) was added to the cultures to ensure plasmid retention. IPTG was added to the medium for  $\beta$ -galactosidase and plasmid-mediated pump inductions. Single-cell efflux assay was carried out as described above in the presence of the various concentrations of the inhibitor, D13-9001.

### Single-cell efflux assay after genetic transformation

The vector plasmid pTH18kr was recombined with the efflux pump gene *tolC* from *S. enterica* (pTH18kr::*tolC*) and introduced into gene-competent  $\Delta$ C cells by electroporation (GenePulser Xcell; BioRad, Japan). The gene-competent cells were prepared without  $\beta$ -galactosidase induction to suppress leakage of  $\beta$ -galactosidase from cell membranes permeabilised during the electroporation process. Then, the transformed cells were cultured in SOC medium containing 1 mM IPTG to induce  $\beta$ -galactosidase and 50  $\mu$ g mL<sup>-1</sup> kanamycin at 37 °C for 3 h, and the single-cell efflux assay was carried out.

### Collection of single droplets containing single cells

Single droplets containing single  $\Delta$ C/pTH18kr::*tolC* cells were collected using a micropipette (inside aperture: 10–15  $\mu$ m) under an optical microscope (IX71; Olympus, Japan) equipped with an objective lens (PlanFluor 20  $\times$ ; Olympus, Japan) and a CCD camera (Neptune 100; Watec, Japan). Images were recorded at 30 frames/s using a digital video recorder (DSR10; Sony, Japan), captured, and sent to a PC by a frame grabber board (Himawari PCI; Library, Japan) as an 8-bit AVI file and analysed using ImageJ software. The micropipette was prepared from a capillary (75  $\mu$ L; Drummond Scientific, USA) using a puller (Model PC10; Narishige, Japan) and microforge (MF900; Narishige, Japan). The micropipette, filled with LB medium and connected to a pressure controller (FemtoJet; Eppendorf, Japan), was manipulated with a micromanipulator (MNM-21; Narishige, Japan). To avoid contamination with cells outside the droplet, the fluorinated oil on the microdroplet array was washed with 70% ethanol before immersing the micropipette in oil. The micropipette was attached to the droplet at a pressure of 50–60 hPa (1 hPa = 100 Pa), and the pressure was decreased to 0 hPa for droplet collection.

### Plasmid analysis

After collecting single droplets containing single cells with a micropipette, the contents of the micropipette were transferred to a test tube containing 2 mL of LB medium supplemented with 50  $\mu$ g mL<sup>-1</sup> kanamycin and cultured overnight at 37 °C. Then, glycerol stock was prepared and stored at -80 °C. The cells were cultured again from the glycerol stock at a later date, and the harboured plasmid was extracted. Using the extracted plasmid as a template, polymerase chain reaction (PCR) was carried out and the amplified DNA fragment was analysed with agarose gel electrophoresis.

## Results and discussion

### Efflux activity of wild-type and efflux pump gene deletion mutant *E. coli* strains

A newly designed hydrophilic-in-hydrophobic micropatterned surface was prepared for bacterial enclosure (Fig. 1A). The diameter of each hydrophilic SiO<sub>2</sub> surface was 10  $\mu$ m, surrounded by a hydrophobic CYTOP layer with a height of 1  $\mu$ m. The CYTOP layer was thicker than that used in a previous study (17 nm).<sup>24</sup> In the newly designed array, droplets were grouped into islands using numbers (Fig. 1A). This facilitated the identification of individual droplets and the cells enclosed in each droplet. More than 300 000 droplets could be prepared simultaneously in a 1 cm<sup>2</sup> area in 1 device by exchanging the cell suspension applied on the hydrophilic-in-hydrophobic micropatterned surface with fluorinated oil. Bacterial cells were enclosed during the droplet formation process (Fig. 1B). Enclosure of the cells was stochastic and dependent on the density of cells in suspension. At the density used in the present study (a turbidity at 600 nm of 0.6), approximately 20–30% droplets contained single cells. For enclosure of bacteria into droplet array formed on the surface, bacterial cells have to be sufficiently close (less than 1  $\mu$ m) to the micropatterned surface. However, in contrast to large eukaryotic cells, small bacterial cells did not settle out easily by gravity and most cells in suspension remained far from the surface. It was difficult to enclose bacteria into droplet array formed on the micropatterned surface with the thin CYTOP layer used in the previous study. We improved this problem by increasing the thickness of CYTOP layer to 1  $\mu$ m. We also assessed the effect of diameter of the hydrophilic surfaces on the number of cells enclosed into each droplet. A larger diameter (20 or 30  $\mu$ m) of hydrophilic surface resulted in an increase of the fraction of droplets containing multiple cells, while the fraction of droplets containing single cell did not increase significantly (not shown). On the other hand, number of droplets formed in 1 device significantly increased when we used hydrophilic surfaces with smaller diameter. Therefore, to increase total number of droplets containing single cells in 1 device, we have applied hydrophilic surface with the diameter of 10  $\mu$ m. To further increase the efficiency of single-cell enclosure, now we are trying to attract the cells to the hydrophilic surface by using dielectrophoresis, which can be achieved by patterning electrodes at the bottom of the hydrophilic surfaces.<sup>28</sup>

The principle of the single-cell drug-efflux assay is shown in Fig. 1C. Wild-type,  $\Delta$ B, and  $\Delta$ C strains of *E. coli* cultured in test

tubes were mixed with FDG and enclosed in a microdroplet array. Upon entering the cytoplasm of *E. coli*, FDG is hydrolysed into a fluorescent dye, fluorescein, by  $\beta$ -galactosidase. We previously confirmed that the strains used in this study expressed comparable levels of  $\beta$ -galactosidase.<sup>12</sup> Both FDG and fluorescein act as substrates for the efflux pump system. In wild-type cells, AcrAB-TolC effectively pumps out FDG, and no fluorescence is observed (Fig. 1C, left). In contrast, FDG is imported into  $\Delta B$  and  $\Delta C$  cells and hydrolysed to fluorescein. In  $\Delta B$  cells, not only cells but also droplets exhibit fluorescence (Fig. 1C, center), because the remaining minor pumps slowly pump out the fluorescein. On the other hand, in  $\Delta C$  cells, fluorescein accumulates in the cell (Fig. 1C, right) because TolC is a common channel protein for both the major and minor resistant-nodulation-division-type efflux pumps expressed in *E. coli*.

Typical images of wild-type,  $\Delta B$ , and  $\Delta C$  cells in the single-cell efflux assay are shown in Fig. 2A. Fluorescence intensities of each cell and the droplet in which the cell was enclosed were measured (Fig. 2B). Wild-type cells and their droplets showed almost no fluorescence, whereas  $\Delta B$  cells exhibited a slight increase in both cell and droplet fluorescence intensities, and  $\Delta C$  cells exhibited high fluorescence intensity within the cell. The fluorescence intensity distributions of the wild-type,  $\Delta B$ , and  $\Delta C$  strains were distinct from each other. As shown in Fig. 2A and B, by enclosing *E. coli* in a femtoliter droplet, weak efflux activity of the  $\Delta B$  cell can easily be detected as fluorescence intensity from both the cell and the droplet (Fig. 2A, enhanced fluorescence images). However, for simplicity, only the cell fluorescence

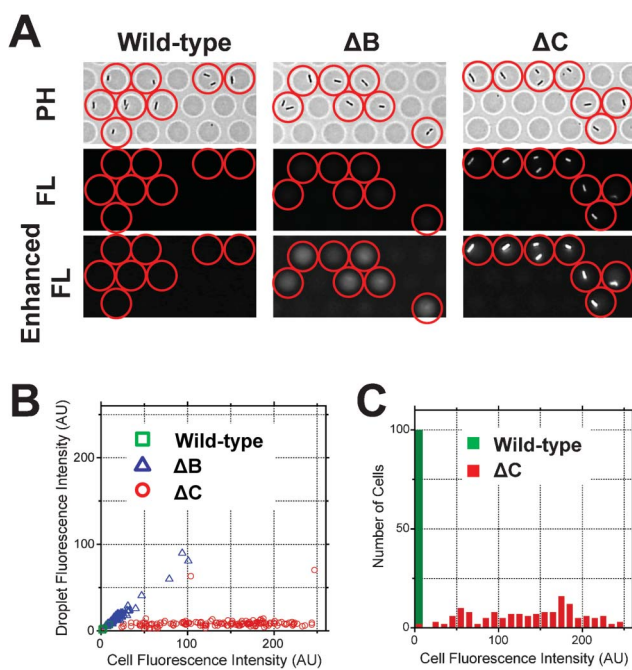


**Fig. 2** Single-cell drug efflux assay on wild-type,  $\Delta B$ , and  $\Delta C$  *E. coli* strains. (A) Phase contrast (PH, top), fluorescence (FL, middle) and enhanced fluorescence (bottom) images of droplets and cells. Droplets containing cells are indicated by red circles. (B) Correlation between cell and droplet fluorescence intensity. (C) Distributions of cell fluorescence intensity.

intensity distribution is discussed in the following experiments (Fig. 2C).

Cells of the  $\Delta C$  strain exhibited large variations in cell fluorescence intensity. Our preliminary result showed that FDG influx into the cell is dependent on the proton-motive force across the cell membrane, suggesting the existence of an FDG importer protein. The variations in cell fluorescence intensity may reflect the expression levels of this as yet unidentified importer protein.

### Effect of the inhibitor on the efflux pump

The effect of an efflux pump inhibitor, D13-9001,<sup>26</sup> was investigated (Fig. 3). D13-9001 has been reported to enhance the antibacterial activities of several antibiotics. A  $\Delta B\Delta C$  double-knockout strain stably expressing MexAB-OprM from *P. aeruginosa* was generated, because *P. aeruginosa* does not have a  $\beta$ -galactosidase-encoding gene. This strain did not emit fluorescence, indicating that the exogenously expressed MexAB-OprM worked well in *E. coli* and the cells recovered

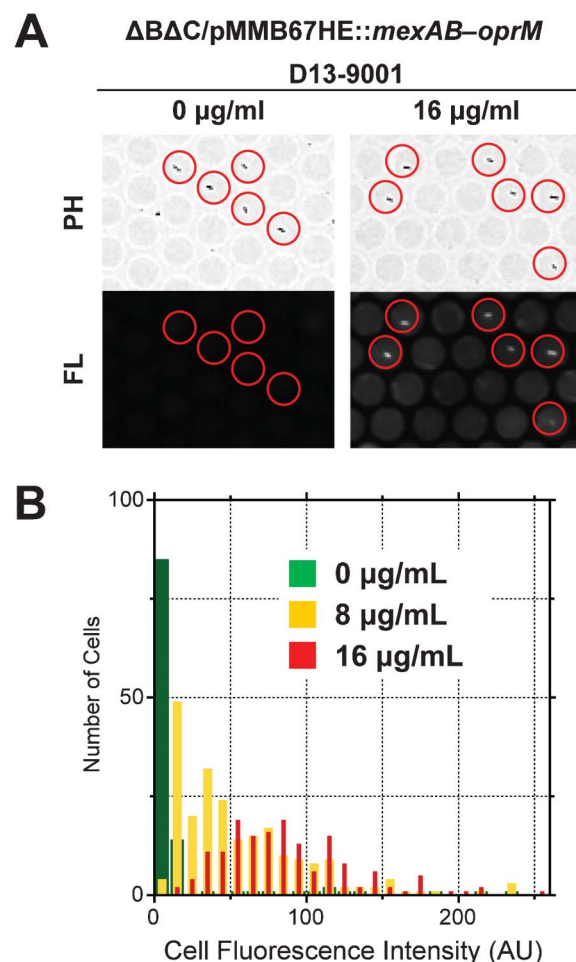


**Fig. 3** Effect of pump inhibitor D13-9001 on the efflux activity of MexAB-OprM expressed in the  $\Delta B\Delta C$  *E. coli* strain. (A) Phase contrast (PH, top) and fluorescence (FL, bottom) images at 0  $\mu\text{g mL}^{-1}$  (left) or 16  $\mu\text{g mL}^{-1}$  (right) D13-9001. Droplets containing cells are indicated by red circles. (B) Distributions of cell fluorescence intensity at different concentrations of D13-9001.

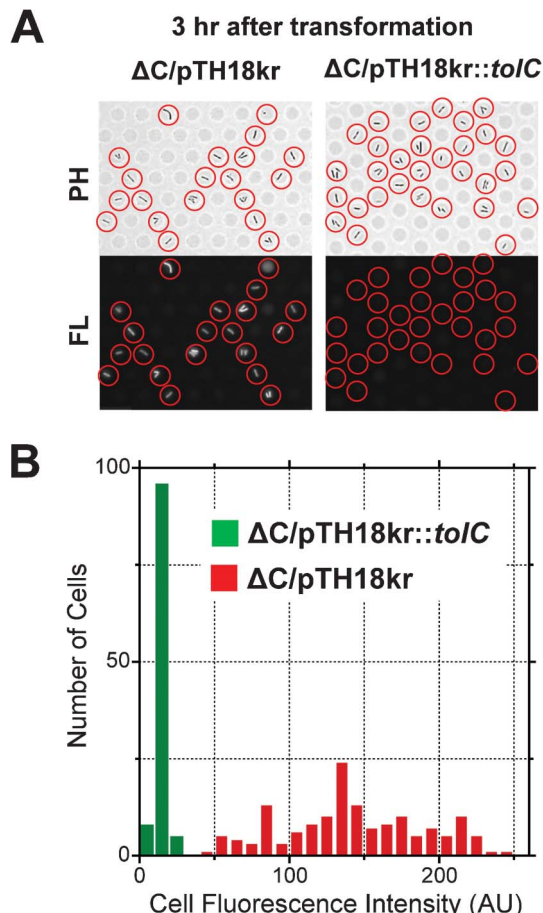
drug efflux activity (Fig. 3A, left). Addition of D13-9001 elicited an increase in the number of fluorescent cells (Fig. 3A, right). As the concentration of D13-9001 increased from  $8 \mu\text{g mL}^{-1}$  to  $16 \mu\text{g mL}^{-1}$ , the fluorescence intensity of cells increased (Fig. 3B), indicating a concentration-dependent inhibitory effect.

The combinatorial use of efflux pump inhibitors with available antibiotics could be effective in treating infections caused by multi-drug resistant bacteria. D13-9001 is known to be a specific inhibitor of MexB, a major efflux pump from *P. aeruginosa*, but it does not inhibit MexY, another major efflux pump from *P. aeruginosa*.<sup>26</sup> MexY inhibitors have not been identified yet. Our approach will be useful to screen for new inhibitors effective against MexY. To screen for inhibitors, numerous compounds have to be tested. In conventional screening, effect of combinatorial use of a compound with antibiotics on the growth of the cell is assessed. The conventional method is not only indirect but also time-consuming because it requires overnight culture before obtaining the results. In contrast, our method is a direct evaluation of efflux activity and takes only 20–30 min. Advantage of our method over conventional one is evident. Furthermore, we have previously shown the microinjection of solution into individual droplet.<sup>24</sup> High-throughput analysis using a droplet array in a device can be realised by developing an automated micropipetting system that is compatible with our device and injects different compounds into subsets of droplets containing bacteria.

#### Appearance of efflux-active phenotype after genetic transformation

To screen for genes encoding drug efflux pumps with rapidity, the efflux assay must be carried out soon after genetic transformation. We examined the time required to recover the efflux-active phenotype by introducing the *S. enterica* *tolC* gene into the  $\Delta C$  cells of *E. coli*. After electroporation with the expression vector pTH18kr::*tolC*, cells were incubated for different durations in the presence of the selection marker kanamycin and the  $\beta$ -galactosidase inducer IPTG. Then, drug efflux activity was assessed using the droplet array. As shown in Fig. 4, the efflux-active phenotype appeared in 3 h. In the control experiment with a vector lacking *tolC* (pTH18kr), no phenotypic change was observed.

One drawback of our efflux assay is the apparent efflux-active signal (low fluorescence intensity of the cell) of the control sample after incubation of less than 3 h, due to a low level of  $\beta$ -galactosidase expression. In our assay,  $\beta$ -galactosidase was induced during the culture period after electroporation. Therefore, the time required for  $\beta$ -galactosidase induction is one of the rate-limiting factors of the assay. In *E. coli*,  $\beta$ -galactosidase expression, which is under the control of the *lac* operon, exhibits an all-or-none behaviour (*i.e.* no expression or high expression).<sup>29,30</sup> In gene-competent cells expressing high levels of  $\beta$ -galactosidase, the electroporation process caused  $\beta$ -galactosidase to leak out of the cell due to transient formation of pores in the cell membrane. This significantly increased the fluorescence intensity of the medium and made the assay difficult. Therefore, prompt induction of  $\beta$ -galactosidase may further shorten the time required to detect a clear phenotypic change.

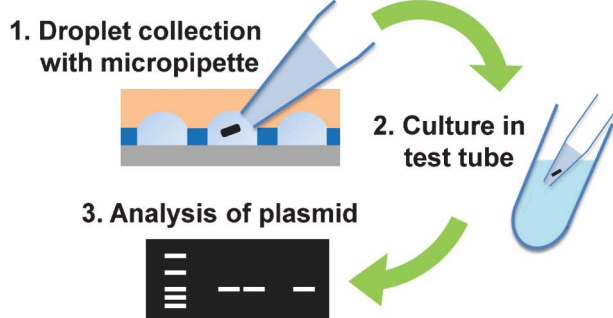
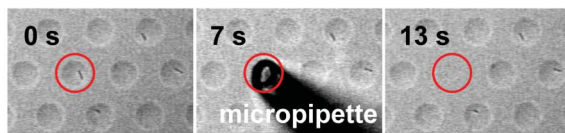
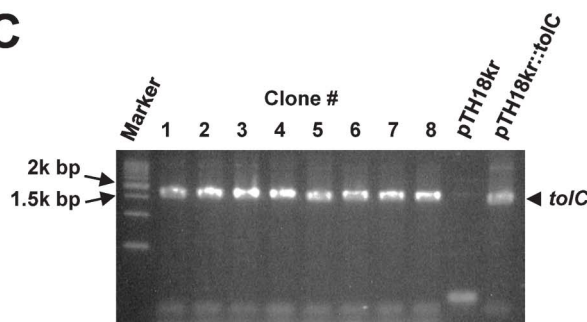


**Fig. 4** Appearance of the efflux-active phenotype after genetic transformation of the  $\Delta C$  *E. coli* strain with plasmid mediated *tolC* from *S. enterica*. (A) Phase contrast (PH, top) and fluorescence (FL, bottom) images of cells transformed with the control vector pTH18kr (left) or vector expressing TolC from *S. enterica* (pTH18kr::*tolC*) (right). Droplets containing cells are indicated by red circles. (B) Distributions of cell fluorescence intensity.

#### Collection of single droplets containing single cells and genotype analysis

One prominent feature of our femtoliter-droplet array is its accessibility to individual droplets from the outside. Collection, addition, and exchange of aqueous content for each droplet are possible by attaching a micropipette and changing the pressure inside the micropipette.<sup>24</sup> We collected single droplets containing single  $\Delta C$  cells expressing TolC from *S. enterica* (Fig. 5). By using a micropipette with an aperture diameter of  $10\text{--}15 \mu\text{m}$ , not only droplets but also cells inside droplets were successfully collected (Fig. 5B). The collected single cells exhibited multiple divisions after transfer to growth medium in a test tube. The plasmid harboured by the divided cells was extracted and used as a template for PCR amplification to determine if the *tolC* gene was retained. The DNA fragment corresponding to the *tolC* gene was detected in all the single cells collected ( $n = 8$  cells) (Fig. 5C).

In the present study, we cultured the collected single cells to increase the number of cells and the harboured plasmids. This process can be omitted by performing DNA amplification with

**A****B****C**

**Fig. 5** Plasmid analysis after the collection of droplets containing single cells. (A) Schematic drawing of the experimental procedure. (B) Sequential images of droplet collection. The collected droplet containing a single cell is indicated by a red circle. (C) Agarose gel electrophoresis of the PCR product amplified using the extracted plasmid as a template. Eight single bacterial cells were collected and analysed.

single-cell PCR.<sup>21</sup> Our system can also be combined with single-DNA analysis in microchamber using loop-mediated isothermal amplification.<sup>31</sup> With the rapid phenotypic change observed after genetic transformation, single-cell gene analysis will enable high-throughput screening.

## Conclusions

A water-in-oil, directly accessible femtoliter-droplet array was successfully applied to assess the drug efflux activity of single bacteria. The inhibitory effect of a chemical compound on the exogenously expressed efflux pump system was easily detected. In future studies, we will attempt to screen for inhibitors of the *P. aeruginosa* MexY pump using this assay system. Furthermore, with the advantage of accessibility, single bacterial cells exhibiting the efflux-active phenotype can be easily collected and used for subsequent genotype analysis. Using a plasmid library of cloned genomic fragments from *S. enterica*, we are now attempting to screen for genes encoding functional efflux pump systems. We believe that our approach will aid in overcoming infectious diseases caused by multidrug-resistant bacteria.

Finally, directly accessible femtoliter-droplet arrays can also be used in other imaging-based phenotypic analyses of single bacteria, such as fluorescence-based proteome and transcriptome analysis of gene expression.<sup>32</sup> We would like to analyse the correlation between gene expression and the emergence of "persister" bacteria that are tolerant to antibiotics despite having the same genotype as normal and sensitive cells.<sup>19,33</sup> In our preliminary experiments, a very small number of *P. aeruginosa* cells exhibited multiple divisions in the femtoliter droplet array after treatment with a high concentration of antibiotics, indicating the existence of persister cells.

## Acknowledgements

We thank Megumi Yamauchi and Mayu Hara for their technical help. This research was partly supported by the Program for Promotion of Fundamental Studies in Health Sciences of the National Institute of Biomedical Innovation, Japan (project ID: 07-3) and the Japan Science and Technology Agency for Core Research for Evolutional Science and Technology (CREST).

## References

- 1 H. Nikaido, *Annu. Rev. Biochem.*, 2009, **78**, 119–146.
- 2 H. Nikaido and Y. Takatsuka, *Biochim. Biophys. Acta, Proteins Proteomics*, 2009, **1794**, 769–781.
- 3 K. Nishino and A. Yamaguchi, *IUBMB Life*, 2008, **60**, 569–574.
- 4 H. I. Zgurskaya and H. Nikaido, *J. Mol. Biol.*, 1999, **285**, 409–420.
- 5 S. Murakami, R. Nakashima, E. Yamashita, T. Matsumoto and A. Yamaguchi, *Nature*, 2006, **443**, 173–179.
- 6 V. Koronakis, A. Sharff, E. Koronakis, B. Luisi and C. Hughes, *Nature*, 2000, **405**, 914–919.
- 7 Y. Morita, N. Kimura, T. Mima, T. Mizushima and T. Tsuchiya, *J. Gen. Appl. Microbiol.*, 2001, **47**, 27–32.
- 8 D. M. Livermore, *Clin. Infect. Dis.*, 2002, **34**, 634–640.
- 9 D. Hocquet, P. Nordmann, F. El Garch, L. Cabanne and P. Plesiat, *Antimicrob. Agents Chemother.*, 2006, **50**, 1347–1351.
- 10 D. Hocquet, M. Roussel-Delvallez, J. D. Cavallo and P. Plesiat, *Antimicrob. Agents Chemother.*, 2007, **51**, 1582–1583.
- 11 B. Henrichfreise, I. Wiegand, W. Pfister and B. Wiedemann, *Antimicrob. Agents Chemother.*, 2007, **51**, 4062–4070.
- 12 Y. Matsumoto, K. Hayama, S. Sakakihara, K. Nishino, H. Noji, R. Iino and A. Yamaguchi, *PLoS One*, 2011, **6**, e18547.
- 13 R. Iino, K. Nishino, H. Noji, A. Yamaguchi and Y. Matsumoto, *Front. Microbiol.*, 2012, **3**, 40.
- 14 R. Nakashima, K. Sakurai, S. Yamasaki, K. Nishino and A. Yamaguchi, *Nature*, 2011, **480**, 565–569.
- 15 G. W. Li and X. S. Xie, *Nature*, 2011, **475**, 308–315.
- 16 C. E. Sims and N. L. Allbritton, *Lab Chip*, 2007, **7**, 423–440.
- 17 K. Gupta, D. H. Kim, D. Ellison, C. Smith, A. Kundu, J. Tuan, K. Y. Suh and A. Levchenko, *Lab Chip*, 2010, **10**, 2019–2031.
- 18 S. Lindstrom and H. Andersson-Svahn, *Lab Chip*, 2010, **10**, 3363–3372.
- 19 N. Q. Balaban, J. Merrin, R. Chait, L. Kowalik and S. Leibler, *Science*, 2004, **305**, 1622–1625.
- 20 L. Cai, N. Friedman and X. S. Xie, *Nature*, 2006, **440**, 358–362.
- 21 E. A. Ottesen, J. W. Hong, S. R. Quake and J. R. Leadbetter, *Science*, 2006, **314**, 1464–1467.
- 22 D. B. Weibel, W. R. Diluzio and G. M. Whitesides, *Nat. Rev. Microbiol.*, 2007, **5**, 209–218.
- 23 J. Q. Boedicker, M. E. Vincent and R. F. Ismagilov, *Angew. Chem., Int. Ed.*, 2009, **48**, 5908–5911.
- 24 S. Sakakihara, S. Araki, R. Iino and H. Noji, *Lab Chip*, 2010, **10**, 3355–3362.
- 25 K. Nishino, Y. Senda and A. Yamaguchi, *J. Infect. Chemother.*, 2008, **14**, 23–29.

26 K. Yoshida, K. Nakayama, M. Ohtsuka, N. Kuru, Y. Yokomizo, A. Sakamoto, M. Takemura, K. Hoshino, H. Kanda, H. Nitanai, K. Namba, Y. Imamura, J. Z. Zhang, V. J. Lee and W. J. Watkins, *Bioorg. Med. Chem.*, 2007, **15**, 7087–7097.

27 V. V. Mokhonov, E. I. Mokhonova, H. Akama and T. Nakae, *Biochem. Biophys. Res. Commun.*, 2004, **322**, 483–489.

28 S. H. Kim, T. Yamamoto, D. Fourmy and T. Fujii, *Biomicrofluidics*, 2011, **5**, 24114.

29 A. Novick and M. Weiner, *Proc. Natl. Acad. Sci. U. S. A.*, 1957, **43**, 553–566.

30 E. M. Ozbudak, M. Thattai, H. N. Lim, B. I. Shraiman and A. Van Oudenaarden, *Nature*, 2004, **427**, 737–740.

31 L. Lam, S. Sakakihara, K. Ishizuka, S. Takeuchi, H. F. Arata, H. Fujita and H. Noji, *Biomed. Microdevices*, 2008, **10**, 539–546.

32 Y. Taniguchi, P. J. Choi, G. W. Li, H. Chen, M. Babu, J. Hearn, A. Emili and X. S. Xie, *Science*, 2010, **329**, 533–538.

33 K. Lewis, *Annu. Rev. Microbiol.*, 2010, **64**, 357–372.